ADVANCED MATERIALS INTERFACES
www.advmatinterfaces.de

Multivalent Bacteria Binding by Flexible Polycationic Microsheets Matching Their Surface Charge Density

*Rameez Ahmed, Ankita Vaishampayan, Jose Luis Cuellar-Camacho, Darren J. Wight, Ievgen Donskyi, Wolfgang Unger, Elisabeth Grohmann, Rainer Haag, and Olaf Wagner**

Aiming at the overall negative surface charge of bacteria, a new strategy of antibacterial agents based on large polymer-modified graphene oxide (GO) sheets is assessed. The presented flexible, polycationic sheets match the size and charge density of the *Escherichia coli* surface charge density (2×10^{14} cm^{-2}). These matching parameters create an unspecific but very strong bacteria adsorber by multivalent, electrostatic attraction. Their interaction with bacteria is visualized via atomic force and confocal microscopy and shows that they effectively bind and wrap around *E. coli* cells, and thereby immobilize them. The incubation of Gram-negative and -positive bacteria (*E. coli* and methicillin-resistant *Staphylococcus aureus*, MRSA) with these polycationic sheets leads to the inhibition of proliferation and a reduction of the colony forming bacteria over time. This new type of antibacterial agent acts in a different mode of action than classical biocides and could potentially be employed in medicinal, technical, or agriculture applications. The presented microsheets and their unspecific binding of cell interfaces could further be employed as adsorber material for bacterial filtration or immobilization for imaging, analysis, or sensor technologies.

1. Introduction

Pathogenic bacteria remain an important medical and scientific challenge for society. Apart from the development of chemical drugs like antibiotics, new strategies to fight bacteria are currently being developed by targeting pathogens physically via nanotechnology.[1–3] Bacteria are dependent on making contact with other surfaces during the first phase of an infection or colony formation.[4] Blocking bacterial surfaces results in their inhibition and ultimately in nonproliferation.[5]

Graphene materials have been shown to act as antibacterial compounds by blocking the bacteria surface.[6,7] They are flexible, nano- or micrometer-sized sheets that can be employed as basis material for various 2D macromolecular architectures. Graphene oxide (GO) is the most commonly used 2D material, as it is the oxidized and exfoliated product from the low-cost resource graphite. GO is not a defined molecule but a collective term for oxidized graphene sheets.[8] The properties of these macromolecular structures are defined by many variable parameters: sheet size, oxidation degree, shape, number of aggregated layers, etc. Therefore, a huge variety of properties for different GO batches is possible. These variable properties can lead to various effects on bacterial cells.[9,10] The reported antibacterial mechanisms of GO include chemical damage via oxidative stress,[11] physical damage from sharp edges,[12,13] extraction of lipid molecules via attracting, and disruptive forces[12,14] or wrapping and trapping by 2D sheets.[6,7] GO can also be employed as a 2D carrier for biocidal compounds that are loaded onto the sheets (e.g., silver,[15,16] zinc oxide,[17,18] iron oxide,[19] or titanium dioxide[20]). Furthermore, IR-laser irradiation after GO sheet binding has been shown to heat up the material as well as the bacterial cell, leading to immediate bacterial cell death.[19,21]

In order to optimize the targeting function of the GO carrier, several research groups have enhanced the binding affinity to bacteria by introducing chemical binding moieties onto the GO sheets (for example, mannose,[22,23] lactose,[23] neutral amines,[23–25] or cationic quaternary amines).[26,27] However, the number of studies on graphene derivatives binding bacteria is still relatively low, compared to the vast number of variable property parameters (lateral size, concentration, exposure time, or bacteria cell

R. Ahmed, Dr. J. L. Cuellar-Camacho, Dr. I. Donskyi, Prof. R. Haag, Dr. O. Wagner
Freie Universität Berlin
Institute of Chemistry and Biochemistry
Takustr. 3, Berlin 14195, Germany
E-mail: olaf.wagner@fu-berlin.de
A. Vaishampayan, Prof. E. Grohmann
Beuth Hochschule für Technik
Seestraße 64, Berlin 13347, Germany
Dr. D. J. Wight
Freie Universität Berlin
Institute of Virology
Robert-von-Ostertag Str. 7-13, Berlin 14163, Germany
Dr. I. Donskyi, Prof. W. Unger
Bundesanstalt für Materialforschung
Unter den Eichen 44-46, Berlin 12203, Germany
The ORCID identification number(s) for the author(s) of this article can be found under https://doi.org/10.1002/admi.201902066.

DOI: 10.1002/admi.201902066

type) that define the experimental outcome.[9,10,28] Therefore, it is crucial to precisely determine and adjust the 2D material parameters to match the bacterial counterpart that should be bound. A universal binding strategy should cover several bacteria cell types including those of different cell shape (e.g., spherical or rodlike) and cell surface composition. A physical property that almost all bacteria share (including Gram-positive and Gram-negative bacteria) is their overall negative surface charge[29] due to the high number of phosphate groups on their surface. Positively charged surfaces can therefore immobilize a wide variety of bacteria via an electrostatic attraction mechanism.[30] It has been shown that surfaces with the exact same charge density of opposing charges ($\approx 10^{14}$ cm^{-2}) not only bind bacteria but also impose a rapid cell death.[31–33] Transferring this concept onto flexible sheets that can further adapt to the pathogen surface, could potentially create a new class of antibiotics that block the pathogen surface and prevent infection or proliferation.

Therefore, we aimed to design a universal counterpart to bacteria surfaces to meet their physicochemical properties as a flexible 2D sheet. As GO is negatively charged, due to its hydroxyl and carboxyl groups, it would repulse bacteria[34] and the surface charge of the sheets needs to be switched to positive. To realize this macromolecular "umpolung," polycationic polymer chains were grafted to the GO sheets. This adds further flexibility as the positive charges in the polymer chains can also move to find their negatively charged counterparts on the bacterial surface. *Escherichia coli* (*E. coli*) and methicillin-resistant *Staphylococcus aureus* (MRSA) were used in incubation experiments to evaluate the effect of flexible polycationic sheets on bacteria cells. By aiming at a general property of bacteria interfaces we assess a new strategy for antibacterial agents that could physically capture and inactivate bacterial cells.

2. Results

2.1. Synthesis and Characterization

2.1.1. Starting Material Property Analysis

In order to achieve the best interaction between GO sheets and bacteria, they should be of same size and charge density. This means that the average lateral size of GO sheets should be in the range of 1–5 µm to suitably interact with bacteria such as *Escherichia coli* (*E. coli*; ≈2 µm). Therefore, micrometer-sized GO sheets were purchased as a starting material that could be directly dispersed and chemically modified. In order to avoid hydrophobic interaction effects and sheet aggregation, the GO raw material was chosen with a high oxidation degree of ≈48 wt% and a C=C to C—O ratio of 2:1 (see elemental analysis, EA, Table S1 and highly resolved C1s X-ray photoelectron spectroscopy (XPS), Figure S5 in the Supporting Information). To determine the average size of the GO flakes scanning electron microscopy (SEM) images (Figure S1, Supporting Information) were acquired and analyzed with ImageJ software. The average lateral size was determined to be 3.0 ± 2.4 µm (Figure S2, Supporting Information). 86% of the sheets had a size in between 0.5 and 5 µm and therefore fit well to the typical size range of bacteria.

2.1.2. Polymer Grafting onto GO and Subsequent Amine Quaternization

The cationic polymer-functionalized GO sheets were prepared via a two-step synthesis. First, the methacrylate polymer chains were introduced by a radical "grafting from" polymerization based on the work of Kan et al.[35] who reported a high polymer density for several methacrylate monomers via free radical polymerization on GO. After the polymer grafting, positive charges were introduced via methylation of the dimethylamines to form quaternary ammonium groups, as shown in Figure S3 (Supporting Information). The detailed synthesis is described in the experimental section. To verify the grafting process and determine the amount of grafted functional groups on GO, EA, XPS, and atomic force microscopy (AFM) were performed. As the GO-starting material contained only traces of nitrogen in its structure (0.01 wt%), the amount of nitrogen was used to determine the polymer functionalization of the dimethylamine polymer. The nitrogen content of the polymer-functionalized GO (GO-poly[2-(dimethylamino)ethyl methacrylate], GO-PDEMA) was determined by EA as 5.5 wt%, which calculates to a degree of polymer functionalization of 62 wt% (**Table 1**).

AFM was used to visualize the functionalization of the GO sheets, as height and surface structure of the polymer-modified

Table 1. Summary of the determined material properties.

Parameter	Numeric value		
Materials	GO	GO-PDEMA	GO-PTEMA
Average lateral size	3.0 ± 2.4 µm	3.0 ± 2.4 µm	3.0 ± 2.4 µm
Average height	1.7 ± 0.18 nm	2.8 ± 0.87 nm	4.78 ± 0.48 nm
Polymer content[a)]	–	62 wt%	62 wt%
Average polymer length[b)]	–	16.4 kDa (104 rep. units ≈25 nm)	16.4 kDa (104 rep. units ≈25 nm)
No. of ammonium groups[c)]	–	–	3.93 mmol g^{-1}
Theoretical charge density[d)]	–	–	8.3×10^{14} cm^{-2} = 8.3 nm^{-2}
Experimental charge density[e)]	–	–	2.3×10^{14} cm^{-2} = 2.3 nm^{-2}
Zeta potential	–39.5 ± 7 mV	+14.5 ± 5 mV	+ 34 ± 4 mV

[a)]Degree of polymer functionalization calculated by elemental analysis; [b)]Molecular weight of polymer chains determined by GPC; [c)]Number of ammonium groups per gram; [d)]Calculated number of charges per unit area; [e)]Experimentally determined number of charges by fluorescein experiment.

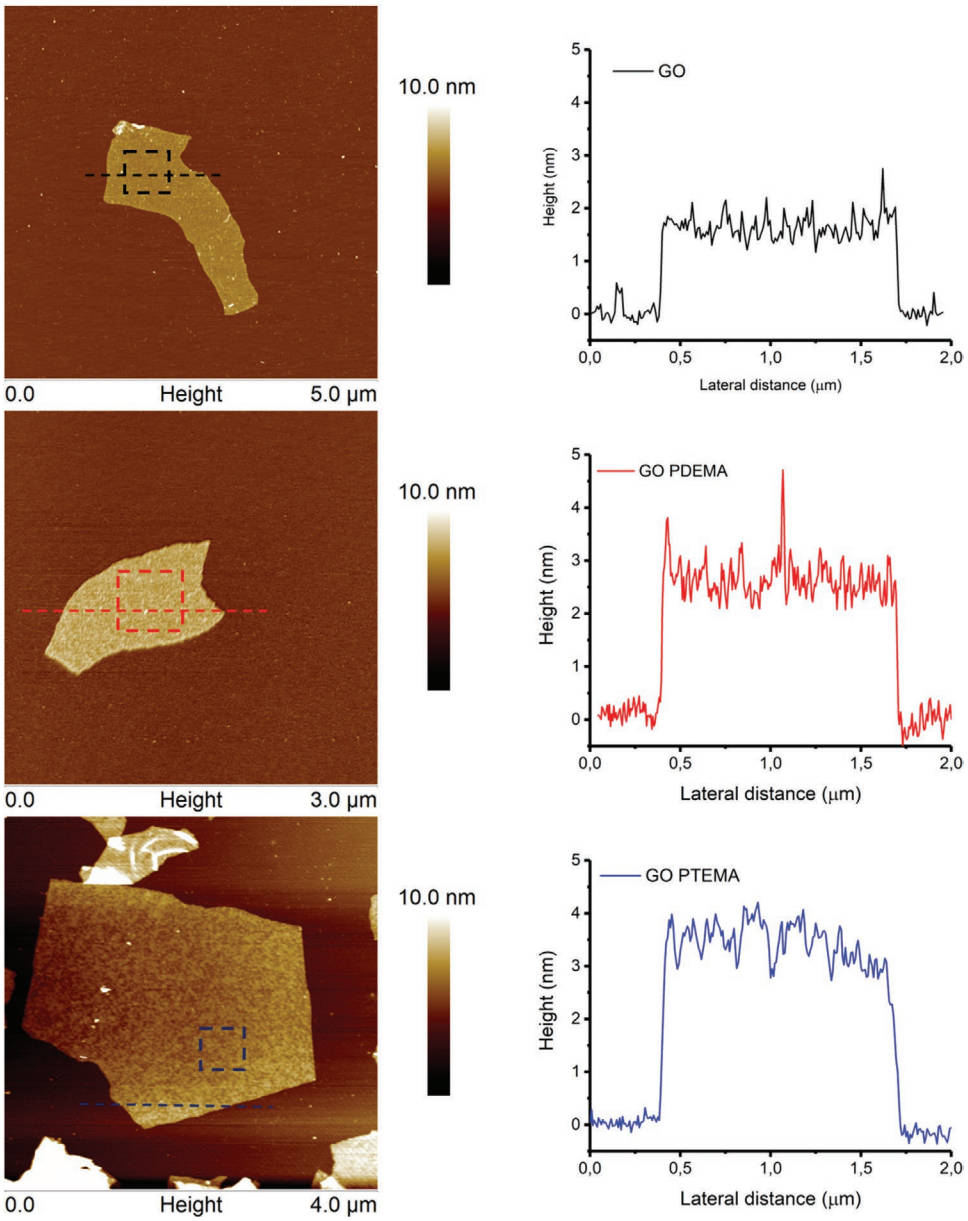

Figure 1. Atomic force microscopy (AFM) images and height profiles of GO, GO-PDEMA, and GO-PTEMA.

GO flakes becomes altered upon functionalization (**Figure 1**). The AFM images show that the GO sheets have a height of ≈1.7 nm, which is typical for GO flakes, and that the polymer-modified GO-PDEMA has a height of ≈2.8 nm. The quaternized sheets with positive charges (GO-poly[2-trimethylammoniumethyl methacrylate chloride] (GO-PTEMA)) were measured and shown to have a height of ≈3.7 nm, suggesting further modification had occurred. The average sheet thickness of GO-PTEMA was determined by measuring twenty sheets by AFM, which gave an average height of 4.78 ± 0.48 nm. These values confirmed the successful grafting of the polymer chains onto the GO starting material.

The compounds were also analyzed by XPS as shown in Figures S5 and S6 (Supporting Information), which further verified the successful polymer modification. To determine the average polymer chain length of polymer-modified GO, the molecular weight (M_w) of nongrafted free polymer was determined by gel permeation chromatography (GPC). A molecular weight of 16 400 g mol^{-1} was determined, which corresponds to 104 monomers per polymer chain (Figure S7, Supporting Information). With a polymer functionalization of 62 wt% of GO-PDEMA, the amount of dimethylamino groups was calculated as 3.93 mmol g^{-1} (Equation S1, Supporting Information). The theoretical number of dimethylamino groups and therefore charges per surface area of the quaternized GO-PTEMA were calculated as 8.36 nm^{-1} = 8.36 × 10^{14} cm^{-1} (Equations S2 and S3, Supporting Information).

2.1.3. Charge Density Calculation

In order to experimentally assess the surface charge of GO-PTEMA their zeta potential was determined. The zeta potential

of the GO starting material was measured to be –40 ± 7 mV, which can be explained by negatively charged hydroxyl or carboxyl groups. The di-amino polymer-modified GO-PDEMA showed a positive value of +15 ± 6 mV. After methylation in excess by methyl iodide, the neutral dimethylamino groups were converted to positively charged ammonium groups and the zeta potential of GO-PTEMA was measured to be +34 ± 4 mV (Figure S8, Supporting Information; Table 1). Compared to that, the corresponding negative zeta potential values of *E. coli* were reported in literature to be –16 to –47 mV.[30,36]

In order to experimentally quantify the number of positive surface charges per surface area, the materials were evaluated in a dye adsorption experiment with a negatively charged dye (fluorescein sodium salt). The amount of the negatively charged dye binding electrostatically to the positive charges of GO-PTEMA was determined by UV–vis spectroscopy (Figure S9, Supporting Information). This revealed the number of charges per mass of GO-PTEMA and was calculated to be 2.3×10^{14} charges cm^{-2} (Equation S6, Supporting Information). It should be noted that the surface charge density of *E. coli* was reported to be 90 μC cm^{-2},[31] which equals 5×10^{14} cm^{-2} (Table 1). Therefore, the charge density on the GO-PTEMA sheets was in the same order of magnitude as determined for bacteria and therefore promising for investigating their bacterial interaction.

2.2. Bacteria Interaction with GO-PTEMA

2.2.1. Interaction with Life/Dead-Stained E. coli Visualized by Confocal Microscopy

In order to assess the effect of GO-PTEMA on bacteria, we stained *E. coli* with two dyes to identify live (SYTO-9; green) and dead (propidium iodide; red) cells and incubated them with 250 μg mL^{-1} GO and GO-PTEMA. Images of bacterial cells were taken using a confocal microscope and showed no dead cells for the control or the GO-treated bacteria. Only the GO-PTEMA treatment showed red-stained cells, indicating disrupted bacterial cell walls by the GO-PTEMA sheets (**Figure 2**a).

Furthermore, stained *E. coli* cells could be seen moving around under the confocal microscope. *E. coli* BL21 (DE3) are nonmotile bacteria but move by random Brownian motion. In order to visualize if GO-PTEMA could affect this Brownian motion, time-lapse images of the SYTO-9-stained live *E. coli* were captured using a confocal microscope. *E. coli* cells could be seen to move around, when they were left untreated or incubated with 250 μg mL^{-1} GO sheets. Interestingly, treatment with 250 μg mL^{-1} GO-PTEMA completely prevented bacteria from moving, suggesting that they were immobilized by being wrapped inside the polycationic GO-PTEMA sheets, and thus preventing their movement by Brownian motion (Figure 2b). This data was also confirmed over a longer time frame of analysis (Figure S10, Supporting Information).

To quantify this observation, all bacterial tracks (>20 consecutive frames in length) from the time lapse were analyzed and showed that the mean velocity of bacterial movements incubated with GO-PTEMA was much lower than the control (Figure 2c). Taken together, this data suggests that GO-PTEMA binds tightly to bacterial cells and wrapping them as a major part of its antimicrobial effect.

2.2.2. Wrapped E. coli Visualized by AFM

In order to further confirm the wrapping of *E. coli* by the GO-PTEMA sheets, AFM was utilized to study the interaction of bacteria and GO-PTEMA in a fluid chamber. Briefly, live *E. coli* on the slightly negatively charged mica substrates were used after depositing a layer of polycationic poly-L-lysine to ensure immobilized bacteria by electrostatic attraction. In case of the *E. coli* samples incubated with GO-PTEMA sheets, bare mica substrates were used without polycationic poly-L-lysine film. The *E. coli* wrapped in positively charged sheets exhibited a positively charged surface and therefore stuck to the mica substrates without further modification (**Figure 3**). The height profiles of GO-PTEMA-treated and free *E. coli* differed and showed an average height of 687 ± 7 nm for *E. coli* alone and

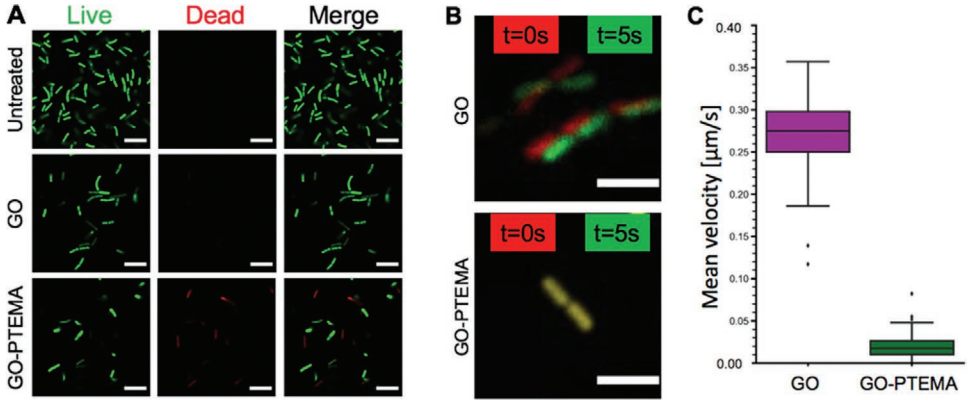

Figure 2. Confocal microscopy of stained and treated *E. coli* BL21 (DE3). *E. coli* were subjected to either no treatment or treatment with GO or GO-PTEMA. Shown are single *z*-plane images of A) *E. coli* stained as live (SYTO-9; green dye) and dead (propidium iodide; red dye) (scale bars equal 10 μm); B) *E. coli* stained with SYTO-9 (green) with time-lapse images with frame 0 (postcolored red) and after 5 s (postcolored green) and then overlaid to show bacterial movement (scale bar = 4 μm); and C) all bacterial tracks (>20 consecutive frames in length) from the time lapse quantified and analyzed. Bar charts show the mean velocity of bacterial movements (GO, nTracks = 65; GO-PTEMA, nTracks = 42).

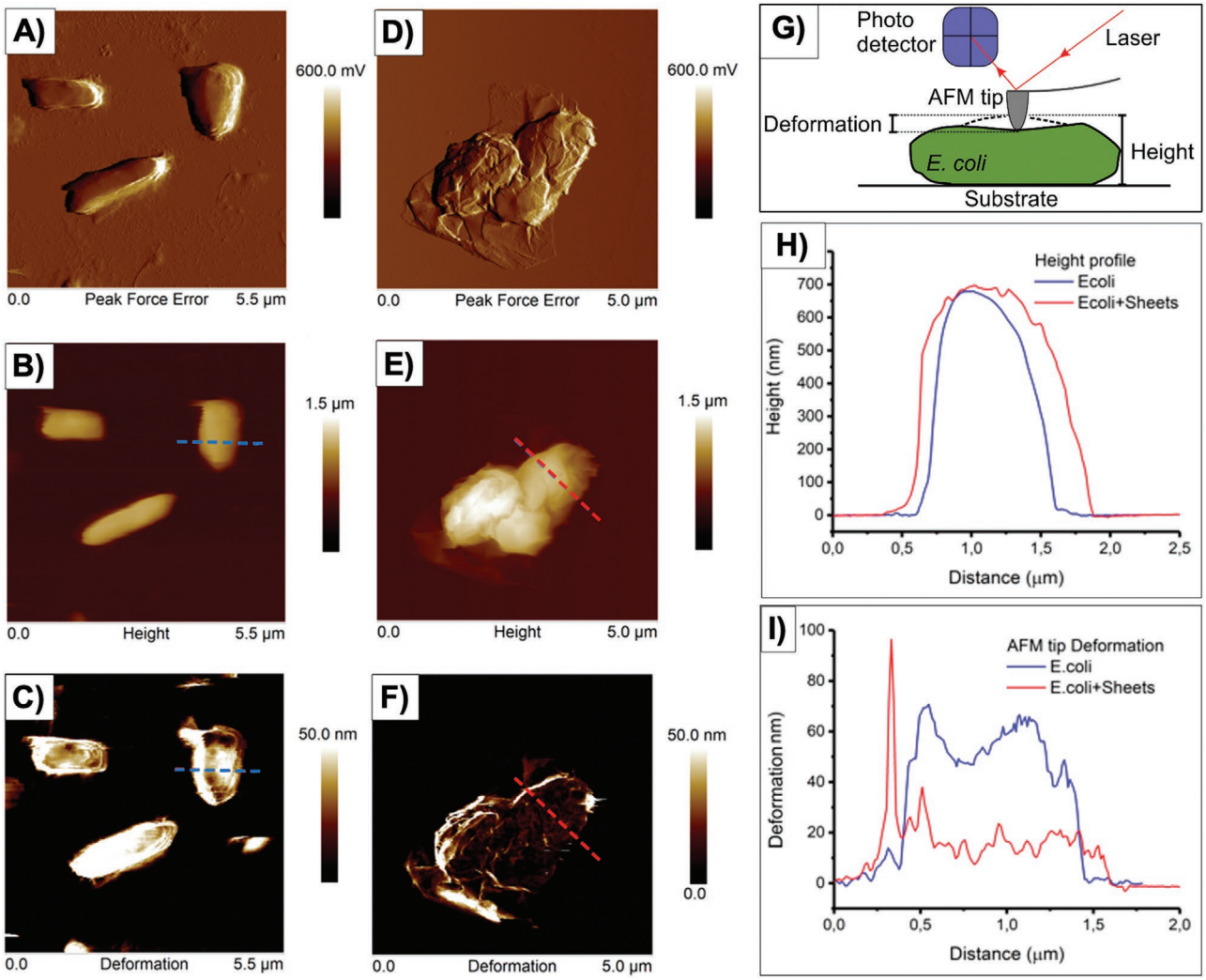

Figure 3. Atomic force microscopy (AFM) images of A–C) *E. coli* and D–F) wrapped *E. coli* after incubation with GO-PTEMA. The height and deformation measurement principle is shown in schematic image (G). Images (A) and (D) are shown in peak force error mode. Images (B) and (E) are shown in height mode. Images (C) and (F) are shown in deformation mode. Images (H) and (I) depict examples of the height and deformation profiles of the free and wrapped *E. coli*.

758 ± 80 nm for *E. coli* with GO-PTEMA. The height difference of ≈70 nm suggests that multiple sheets of 4.8 nm thickness must be wrapped around the bacteria. No wrapping of bacteria could be found for *E. coli* incubated with raw material GO sheets.

Furthermore, the samples were imaged in PeakForce mode under constant maximal loading force by the tip (6 nN). By this nanomechanical mapping method, the deformation profiles obtained for free and treated *E. coli* were compared by the degree of deformation. The samples revealed a clear difference in the induced deformation depth. While the deformation depth of *E. coli* alone was 53.1 ± 3.4 nm, GO-PTEMA-treated *E. coli* seemed to provide a structural reinforcement during indentation by the AFM tip, which led to a decreased deformation depth of 15.8 ± 5.3 nm. Therefore, the deformation profiles obtained for free bacteria and wrapped bacteria could be used to differentiate the two states (Figure 3I).

2.2.3. Growth Inhibition of Gram-Positive and Gram-Negative Bacteria

The antibacterial activity of graphene materials as well as their antibacterial mechanisms have been discussed controversially in many publications.[28] In order to evaluate the antibacterial activity of GO-PTEMA, we conducted incubation and bacterial proliferation experiments. To preclude that toxic compounds, which might have been adsorbed onto the graphene sheets during synthesis, could leach out of the testing materials and thereby kill bacteria, a disc diffusion assay was performed. After 24 h as well as 5 days of incubation, no inhibition zone was observed for the tested materials (GO, GO-PDEMA, and GO-PTEMA), therefore ruling out an antibacterial activity by desorbed toxins (Figure S11, Supporting Information).

The growth inhibition was further tested in liquid phase with varying concentrations of GO, GO-PDEMA, and GO-PTEMA to determine the minimal inhibition concentration (MIC) against

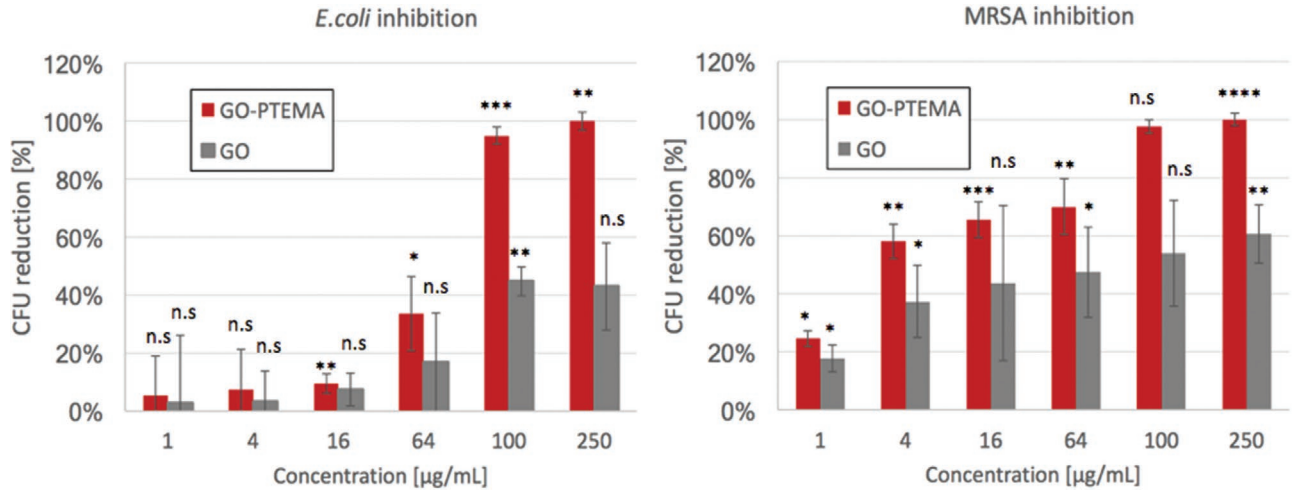

Figure 4. Bacteria inhibition at different concentrations of GO-PTEMA and GO. *E. coli* (Gram-negative) (left) and MRSA (Gram-positive).

E. coli BL21 (DE3) and MRSA (04-02981). Briefly, the effect on bacteria was determined by counting the colony forming units (CFU) on agar plates, which allowed an accurate determination of viable bacterial cells. *E. coli* cultures (CFU = 10^7) were incubated with different concentrations of GO-PTEMA and GO as control. The reduction of the CFU compared to the control (only *E. coli*, without sample) was calculated in percent and is shown in **Figure 4**. It is shown that after 6 h of incubation in growth medium, GO-PTEMA concentrations of 100 µg mL^{-1} and higher resulted in a reduction of the number of *E. coli*, as well as MRSA, of more than 99% compared to the control culture without an antibacterial compound. Furthermore, the antibacterial effect of GO-PTEMA sheets was much stronger compared to GO sheets, even at concentrations of 250 µg mL^{-1} GO could reduce the CFU of both *E. coli* and MRSA by only 60%.

In order to monitor the growth inhibition over time, the above MIC test was repeated with a constant GO or GO-PTEMA concentration of 250 µg mL^{-1}. Briefly, ≈10^5 CFU mL^{-1} *E. coli* or MRSA solution were incubated with the two compounds at 37 °C and samples were taken every 2 h to determine the CFU mL^{-1} by counting the colonies on agar plates. GO-PTEMA showed a significant inhibition of the bacterial growth for both *E. coli* and MRSA. By incubating with 250 µg mL^{-1} of GO-PTEMA the bacterial number reduction is visible after 2 h for both bacteria. For MRSA the CFU shows a 100-fold reduction, which reflects the 5 times lower surface area and thus higher susceptibility to surface blocking compared to *E. coli*.[29] Further incubation time resulted in a slow decrease in CFU values for both bacteria over the period of 6 h, while the control culture as well as the GO-incubated bacteria continued to grow. The GO-incubated bacteria only showed a marginally slower proliferation than the control without any compound. After 6 h incubation the CFU reduction of GO-PTEMA (99.96% *E. coli*; 99.99% MRSA), calculated against the control culture in percent, was much higher than that of GO (60% *E. coli*; 60% MRSA) as shown in **Figure 5**.

2.2.4. Electrostatic Binding Mechanism Test by Salinity-Dependent Growth Inhibition Assay

In order to confirm that the main mechanism of bacterial inhibition is based on electrostatic attraction between the GO-PTEMA and the bacteria, *E. coli* were incubated in medium with increasing sodium chloride (NaCl) concentrations, which changes the ionic strength of the surrounding solution. The binding affinity based on electrostatic interaction of the GO-PTEMA sheets to *E. coli* should therefore decrease and result

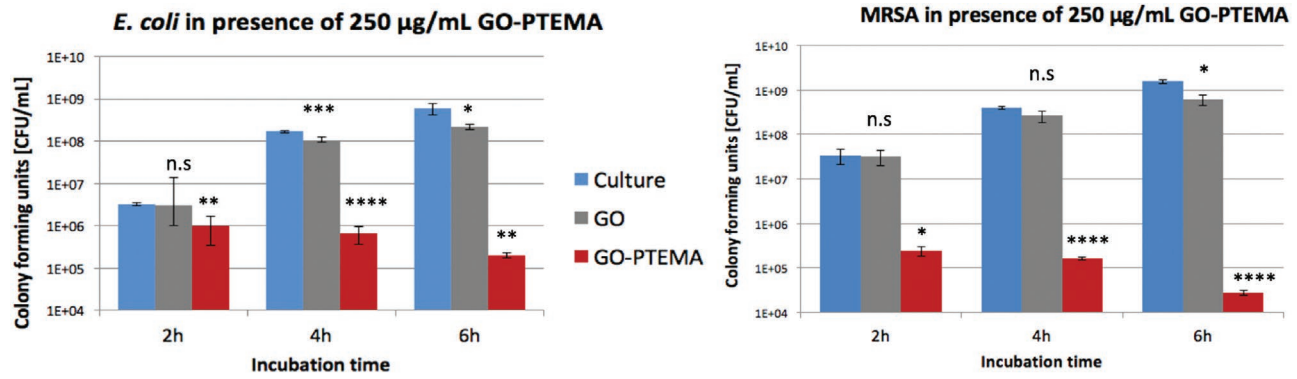

Figure 5. Growth inhibition experiment of MRSA (Gram-positive) and *E. coli* (Gram-negative) bacterium.

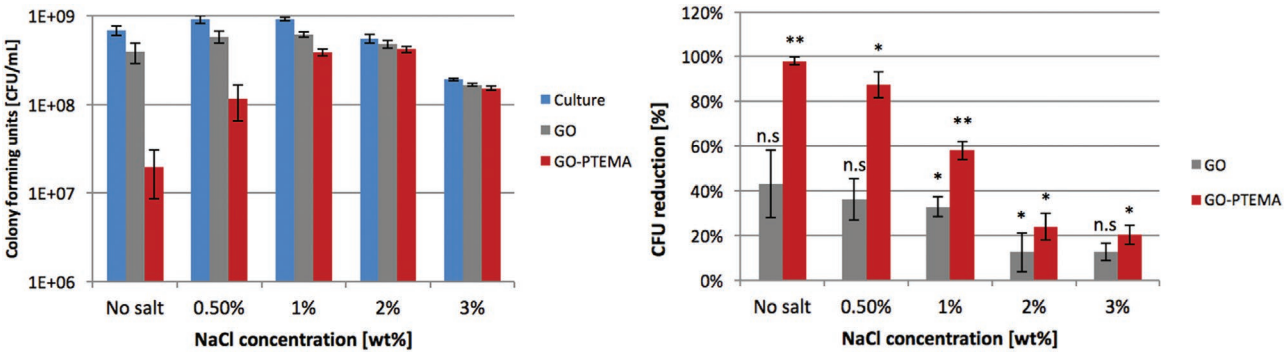

Figure 6. Salinity-dependent growth inhibition. Colony count graph (left) and CFU reduction in percent (right).

in lower bacteria inhibition. Briefly, *E. coli* (10^4 CFU mL^{-1}) were incubated with GO-PTEMA (250 µg mL^{-1}) for 6 h in medium with NaCl concentrations of 0, 0.5, 1, 2, and 3 wt%. The maximum inhibition activity of 99% was observed for the medium without NaCl (0 wt%) (**Figure 6**). An increase in the salt concentration resulted in reduced inhibition activities of 87%, 58%, 24%, and 20%, in the respective order shown above. These results indicate that the electrostatic attraction of GO-PTEMA is the main binding mechanism and cause of bacterial growth inhibition.

Furthermore, as the electrostatic binding mechanism is reversible at high salt concentrations, these polycationic sheets could be used for bacterial enrichment experiments that could be utilized in a number of future studies.

3. Conclusion

We assess a multivalent type of antibacterial agent and presented its design and synthesis based on defined target parameters. These parameters (lateral size and charge) were chosen for optimal bacteria binding and were confirmed by SEM, AFM, zeta potential, and a dye adsorption assay. The charge density of 2×10^{14} cm^{-2} matched the negatively charged bacterial surface density known from literature.[31]

We could show by AFM and confocal microscopy that the GO-PTEMA sheets bind tightly to *E. coli* and wrap around the bacteria cells, thereby immobilizing them. In contrast, this was not the case for the unmodified GO sheets, which did not wrap bacterial cells or inhibited bacteria movement. The incubation of Gram-negative and -positive bacteria (*E. coli* and MRSA) with GO-PTEMA resulted in the inhibition of proliferation and a slow reduction of the number of colony forming bacteria. This effect can be attributed to the observed wrapping of bacteria cells that might result in the blockade of metabolic exchange pathways. The salt concentration dependency of the inhibition experiment, as well as the fact that unmodified negatively charged GO sheets did not inhibit bacteria, confirm that the main driving force of the antibacterial effect is based on electrostatic attraction.

The presented compound binds and wraps bacteria cells, which inhibits proliferation and results in a slow cell death. Therefore, it can be described as an antibacterial agent acting on a different mode of action than classical antibiotics or biocides. Besides the antibacterial property that has potential use in medicinal, technical, or agriculture applications, the multivalent binding could also be applied for adsorbing bacteria or other cell types. The presented GO-PTEMA and its unspecific binding of cell interfaces could be employed as adsorber material for bacterial filtration or immobilization methodology in cell analysis and imaging applications. The graphene-sheet-based immobilization furthermore offers electroconductive materials that can be used to transmit electrical signals in sensor setups.

4. Experimental Section

Materials and Methods: Used chemicals were purchased from following sources: 2-(dimethylamino)ethyl methacrylate (98%, Aldrich), 2,2′-azobis(2-methylpropionitrile) (98%, Aldrich), aluminum oxide (50–200 µm, Acros Organics) 3-dimethylaminopropylamin (99%, Aldrich), methyl iodide (99%, Acros Organics) dimethylformamide (99.5%, Acros Organics), tetrahydrofuran (99.9%, VWR chemicals), fluorescein sodium salt (Sigma-Aldrich), poly-L-lysine (MW 75–150 kDa, from Sigma-Aldrich, LB-Broth or LB-Agar (Carl Roth GmbH & Co. KG, Karlsruhe, Germany). The graphene oxide (GO) sheets were purchased as paste from "graphene-supermarket.com," 0.5–5 µm, 80%).

GO-PDEMA Synthesis: GO was functionalized based on the method reported by Kan et al.[35] 300 mg GO was dispersed in 350 mL of *N*,*N*-dimethylformamide (DMF) in a 500 mL Schlenk flask and sonicated (35 kHz, 160 W) for 30 min. 15.6 g (100 mmol) of DEMA monomer was added to the reaction mixture. The DEMA monomer was previously cleared from the quinoline stabilizer by filtration through 1 g aluminum oxide (ALOX). The reaction mixture was then flushed with nitrogen for 30 min to remove oxygen. Under nitrogen flow protection and constant stirring, 820 mg (5 mmol) of AIBN was added. The reaction mixture was stirred at 65 °C for 48 h. Then it was transferred to 50 mL falcon tubes for purification via centrifugation at 9000 rpm and 15 °C 3–4 times with DMF and 3–4 times with DI water for purification. After extensive purification the product was dispersed in 200 mL DI water and lyophilized to obtain 600 mg of a dry black solid.

GO-PTEMA Synthesis: To introduce permanent positive charges, the dimethylamine groups of GO-PDEMA were methylated to form quaternary ammonium ions.[37] 150 mg GO-PDEMA (0.59 mmol repeating unit) was dispersed in 80 mL THF via 15 min of ultrasonication. Methyl iodide (MeI) (1 mL, 16 mmol) in excess was added under constant stirring for 24 h. The reaction mixture was transferred to 50 mL falcon tubes for purification via centrifugation 3–4 times with THF and 3–4 times with DI water. It was dispersed in 50 mL DI water and lyophilized to obtain 155 mg as a dry black solid.

Scanning Electron Microscopy: The GO sheets were imaged with a field emission scanning electron microscope (FE-SEM, Hitachi SU8030)

at 20 kV, a current of 10 µA and a working distance (WD) of around 8.3. The samples were coated with a gold layer by using a sputter coater (Emscope SC 500, Quorum Technologies, UK).

Atomic Force Microscopy: Imaging of functionalized graphene sheets and their interaction with bacteria was carried out with an atomic force microscope Multimode 8 from Bruker in PeakForce QNM mode (Quantitative NanoMechanics) with a NanoScope V controller. All experiments were performed in a closed fluid chamber in Milli-Q water. The NanoScope software 1.5 from Bruker was used for image analysis where plane fit and flatten tools with order 1 were used. To identify the effective interaction between GO-PTEMA sheets and bacteria, both samples were first imaged independently. Discs of muscovite mica of about 1 cm in diameter were cleaved with regular tape and used as substrates for sample deposition. SNL tips from Bruker were used with nominal radius in the range of 2–12 nm and cantilever spring constant of 0.35 N m^{-1}. Before any imaging was performed, the sensitivity of the cantilever was acquired from a force distance curve after compression on the hard surface of mica and subsequently the thermal noise method was applied to extract its spring constant. Images were taken with a resolution of 512 points per line and 0.7 Hz scan rate.

10 µL of a GO sample (1–3 mg mL^{-1}) was deposited on cleaved mica and allowed to dry. The sample was rinsed repeatedly with Milli-Q water and imaged in a closed chamber. Although it is well known that GO is mostly negatively charged, it was observed that a few flakes remained attached to the surface of cleaved mica when substrate was rehydrated. On the other hand, positively charged functionalized GO sheets (GO-PTEMA) that were precipitously bound on the mica surface were driven by the strong electrostatic interaction to silanol groups present on its surface. For this reason, the original sample concentration was 10-fold diluted before deposition followed by 15 min of incubation. Maximal loading forces during imaging were 0.5–1 nN. Imaging of live bacteria was achieved on cleaved mica substrates after deposition of a layer of a cationic polymer. 5 µL of poly-L-lysine (MW 75–150 kDa, from Sigma-Aldrich) was deposited at the center of cleaved mica and allowed to dry. Afterward, the surface was rinsed with Milli-Q water, allowed again to dry, and used as substrate for deposition of the sample. A sample with *E. coli* BL21 (DE3) was centrifuged at 5000 rpm, the supernatant (culture medium) was removed, and 100 µL of Milli-Q water was added and mixed. Then 15 µL of the prepared sample was deposited at the center of the poly-L-lysine-coated mica and incubated for at least 10 min. After incubation, the sample was slightly blotted with a filter paper to reduce the amount of liquid in the sample to only a very thin film but without allowing to dry. The sample was mounted on the AFM head and the liquid chamber was assembled. Maximum loading forces were optimized to avoid shadowing effects present due to the high bacteria lateral cross section and its interaction with the conical AFM tip. Therefore, maximal loading forces were 6 nN, which were still within the elastic reversible response of the bacterial cell wall and allowed to repeatedly image. Also, this applied force setpoint induced a defined degree of deformation on the cells, which could be easily monitored and further compared with the case of cells trapped within GO-PTEMA sheets, as described below. To monitor the binding of GO-PTEMA sheets with bacteria, bare mica substrates were used, because the wrapped bacteria should have exhibited a positively charged surface compared to nonwrapped bacteria. Imaging conditions were kept constant as in the case of imaging live bacteria. The samples were diluted in a similar ratio as when measured individually. 10 µL of each sample was added to 80 µL of Milli-Q water and incubated for at least 40 min. Finally, 10 µL of the sample with the mixture was deposited at the center of cleaved mica and incubated for 15 min, followed by slight blotting to leave a thin film and then mounted to the AFM head for measurement.

X-Ray Photoelectron Spectroscopy: The gold substrates for XPS analysis were cleaned in a piranha solution (1:4) 30% H_2O_2:98% H_2SO_4 (v/v) during ultrasonication at room temperature for 10 min. Then they were washed with the DI water 5 times and with acetone 2 times. After drying overnight, the studied compounds were dissolved in methanol and evenly distributed dropwise over the surface of gold substrates. Synchrotron XPS was carried out at the high-energy spherical-grating monochromator (HE-SGM) dipole beamline at BESSY II in Berlin, Germany. A fixed analyzer transmission mode at pass energy of 50 eV and the following excitation energies were used: survey scan 750 eV, O 1 s 620 eV, N 1 s 500 eV, and C 1 s 385 eV. The spectra were recorded at an electron emission angle of 60°. All XPS spectra were processed with the UNIFIT program (version 2017). A Gaussian/Lorentzian product function peak shape model GL (30) was used in combination with a Shirley background. If not otherwise denoted, the L–G mixing for component peaks in all spectra was constrained to be identical. Peak fitting of C1s spectra was performed by using an asymmetric peak shape model for the graphene C1s component peak and a symmetric peak shape model for all other component peaks. After peak fitting of the C1s spectra, all the binding energies were calibrated in reference to the graphene C1s' component at a binding energy of 284.6 eV. High-resolution, core-level spectra were recorded in FAT (fixed analyzer transmission) mode at pass energy of 20 eV using excitation energy of 1486.69 eV for all elements: O1s, N1s, and C1s.

Elemental Analysis: EA was carried out on a VARIO EL III instrument (Elementar, Hanau, Germany) using sulfanilic acid as the standard.

Gel Permeation Chromatography: GPC measurements were performed on an Agilent 1100 Series HPLC series, equipped with a PSS SUPREMA 1000 Å providing a separation range from 100 to 1 000 000 Da. Eluent was H_2O + 0.3 M formic acid and calibration was performed with pullulan obtained from PSS. Analysis was performed with WinGPC.

Zeta Potential: The zeta potential measurements were performed by a Malvern Zetasizer Nano machine (Brookhaven Instruments Corp.) at 25 °C. All measurements were performed in disposable capillary cell (DTS1070) from Malvern instruments. 0.1 g mL^{-1} samples in Millipore quality water were used in all the measurements.

Confocal Microscopy: *E. coli* BL21 (DE3) were inoculated into fresh LB culture media to ≈10^4 CFU mL^{-1} and grown for 2 h at 37 °C (180 rpm). The culture was then split into three tubes and treated with i) LB media, ii) GO, or iii) GO-PTEMA at a final concentration of 250 µg mL^{-1}. After 20 min of incubation at 37 °C with shaking (180 rpm) the samples were then stained with BacLight Live/Dead staining kit (ThermoFisher) according to the manufacturer's instructions, resuspended in 50% glycerol and briefly centrifuged onto µ-Slide 8-well chambered cover glass (ibidi). Single Z-plane confocal images were acquired through a ×100 NA1.45 objective on a VisiScope Confocal FRAP System (VisiTron systems). Images were recorded on an iXON 888 EMCCD (Andor) using the same laser intensities, EMCCD gain, and exposures between samples. Images were all processed equally in the Fiji distribution of ImageJ using a custom written IJ1 script.[38] Time-lapse images of the live bacteria on the glass surface were quantified and analyzed.

Disc Diffusion Assay: *E. coli* BL21 (DE3) was prepared in LB-Broth or LB-Agar [Carl Roth GmbH & Co. KG, Karlsruhe] at 37 °C with constant shaking at 150 rpm. Agar diffusion tests were performed according to CLSI guidelines.[39] Bacteria cultures (OD_{600} = 0.2) were distributed with a sterile cotton swab on an agar plate. The Whatman filter paper discs (6 mm diameter) were immersed in corresponding concentrations (2, 4, 8, 16, 32, 64, and 100 µg mL^{-1}) of the test samples and placed on the agar plate. A paper disc was immersed in sterile deionized water as reference. The plates were incubated at 37 °C and checked after 24 h and 5 days.

Bacterial Growth Inhibition Assay (MIC): Due to the turbidity of graphene oxide solutions, all bacteria concentrations were determined by counting the CFU, instead of determining the OD_{600} values. *E. coli* BL21 (DE3) (CFU = 10^7) as well as with *S. aureus* 04-02981 (MRSA) were incubated in LB medium with 0.001 wt% NaCl at 37 °C for 6 h with different concentrations of GO and GO-PTEMA. The reduction of the CFU values compared to the control (only bacteria) was calculated in percent.

Growth Inhibition Assay (Time Dependent): The time-dependent inhibition assay was performed with *E. coli* BL21 (DE3) and *S. aureus* 04-02981 in presence of GO or GO-PTEMA to elucidate the mechanism of action of GO-PTEMA with respect to different incubation times. For this, overnight cultures of *E. coli* and MRSA were prepared in LB broth and tryptic soy broth (TSB) without addition of sodium chloride, respectively. Overnight cultures were incubated at 37 °C with a constant agitation at 150 rpm, subsequently set to ≈10^5 CFU mL^{-1}, and exposed

to 250 μg mL^{-1} of GO or GO-PTEMA in a total volume of 6 mL. The samples were incubated at 37 °C, 150 rpm and samples were taken after 2, 4, and 6 h. The samples were serially diluted and spread on LB agar plates to determine their CFU mL^{-1}. The reduction of the CFU values in percent in presence of GO or GO-PTEMA was calculated with reference to the untreated cultures of *E. coli* and MRSA.

Growth Inhibition Assay (Salinity Dependent): This inhibition assay was performed to determine the susceptibility of *E. coli* BL21 (DE3) to GO and GO-PTEMA at different NaCl concentrations. Overnight cultures of *E. coli* BL21 (DE3) were prepared in LB broth without NaCl and incubated at 37 °C with a constant agitation at 150 rpm, subsequently set to ≈10^4 CFU mL^{-1}, and exposed to 250 μg mL^{-1} of GO or GO-PTEMA at varying NaCl concentrations of 0, 0.5, 1, 2, and 3 wt%. The total volume of each sample was 6 mL. The samples were incubated for 6 h at 37 °C, 150 rpm followed by serial dilution and spreading on LB agar plates to determine the CFU mL^{-1}. The reduction in *E. coli* CFU values in percent in presence of GO or GO-PTEMA was calculated with reference to untreated *E. coli* cultures and is presented in dependence of the sample salinity.

Supporting Information

Supporting Information is available from the Wiley Online Library or from the author.

Acknowledgements

This work was supported by the SFB765 funded by the Deutsche Forschungsgemeinschaft (DFG) and ProFIT funded by Europäische Fonds für regionale Entwicklung (EFRE). The authors also acknowledge support by the team at the BESSY II synchrotron radiation facility as well as Dr. A. Nefedov (Karlsruhe Institute of Technology, KIT) from the HE-SGM Collaborate Research Group. The authors thank their colleagues Andrés Velázquez for artwork and Dr. Pamela Winchester for language polishing.

Conflict of Interest

The authors declare no conflict of interest.

Keywords

antibacterial, *Escherichia coli*, graphene, inhibition, *Staphylococcus aureus*

Received: December 11, 2019
Revised: May 11, 2020
Published online:

[1] P. V. Baptista, M. P. McCusker, A. Carvalho, D. A. Ferreira, N. M. Mohan, M. Martins, A. R. Fernandes, *Front. Microbiol.* **2018**, *9*, 1441.
[2] R. Singh, M. S. Smitha, S. P. Singh, *J. Nanosci. Nanotechnol.* **2014**, *14*, 4745.
[3] L. Rizzello, R. Cingolani, P. P. Pompa, *Nanomedicine* **2013**, *8*, 807.
[4] D. H. Stones, A. M. Krachler, *Biochem. Soc. Trans.* **2016**, *44*, 1571.
[5] G. Y. Zhu, B. Y. Lu, T. X. Zhang, T. Zhang, C. L. Zhang, Y. Li, Q. Peng, *Nanomedicine* **2018**, *13*, 1093.
[6] O. Akhavan, E. Ghaderi, A. Esfandiar, *J. Phys. Chem. B* **2011**, *115*, 6279.
[7] S. Liu, M. Hu, T. H. Zeng, R. Wu, R. Jiang, J. Wei, L. Wang, J. Kong, Y. Chen, *Langmuir* **2012**, *28*, 12364.
[8] A. M. Dimiev, E. Siegfried, *Graphene Oxide: Fundamentals and Applications*, John Wiley & Sons, Ltd, Chichester, West Sussex, UK **2017**.
[9] H. Ji, H. Sun, X. Qu, *Adv. Drug Delivery Rev.* **2016**, *105*, 176.
[10] X. Zou, L. Zhang, Z. Wang, Y. Luo, *J. Am. Chem. Soc.* **2016**, *138*, 2064.
[11] S. Gurunathan, J. W. Han, A. A. Dayem, V. Eppakayala, J.-H. Kim, *Int. J. Nanomed.* **2012**, *7*, 5901.
[12] V. T. Pham, V. K. Truong, M. D. Quinn, S. M. Notley, Y. Guo, V. A. Baulin, M. Kobaisi, R. J. Crawford, E. P. Ivanova, *ACS Nano* **2015**, *9*, 8458.
[13] S. Xiao, X. Lu, L. Gou, J. Li, Y. Ma, J. Liu, K. Yang, B. Yuan, *Carbon* **2019**, *149*, 248.
[14] W. Hu, C. Peng, W. Luo, M. Lv, X. Li, D. Li, Q. Huang, C. Fan, *ACS Nano* **2010**, *4*, 4317.
[15] J. Tang, Q. Chen, L. Xu, S. Zhang, L. Feng, L. Cheng, H. Xu, Z. Liu, R. Peng, *ACS Appl. Mater. Interfaces* **2013**, *5*, 3867.
[16] J. Ma, J. Zhang, Z. Xiong, Y. Yong, X. S. Zhao, *J. Mater. Chem.* **2011**, *21*, 3350.
[17] Y. -W. Wang, A. Cao, Y. Jiang, J. -H. Liu, Y. Liu, H. Wang, *ACS Appl. Mater. Interfaces* **2014**, *6*, 2791.
[18] L. Zhong, K. Yun, *Int. J. Nanomed.* **2015**, *10*, 79.
[19] W. Y. Pan, C. C. Huang, T. T. Lin, H. Y. Hu, W. C. Lin, M. J. Li, H. W. Sung, *Nanomedicine* **2016**, *12*, 431.
[20] Y. N. Chang, X. M. Ou, G. M. Zeng, J. L. Gong, C. H. Deng, Y. Jiang, J. Liang, G. Q. Yuan, H. Y. Liu, X. He, *Appl. Surf. Sci.* **2015**, *343*, 1.
[21] Z. Qi, P. Bharate, C. H. Lai, B. Ziem, C. Böttcher, A. Schulz, F. Beckert, B. Hatting, R. Mülhaupt, P. H. Seeberger, R. Haag, *Nano Lett.* **2015**, *15*, 6051.
[22] W. Zhan, T. Wei, L. Cao, C. Hu, Y. Qu, Q. Yu, H. Chen, *ACS Appl. Mater. Interfaces* **2017**, *9*, 3505.
[23] P. Subramanian, F. Barka-Bouaifel, J. Bouckaert, N. Yamakawa, R. Boukherroub, S. Szunerits, *ACS Appl. Mater. Interfaces* **2014**, *6*, 5422.
[24] K. H. Tan, S. Sattari, I. S. Donskyi, J. L. Cuellar-Camacho, C. Cheng, K. Schwibbert, A. Lippitz, W. E. S. Unger, A Gorbushina, M. Adeli, R. Haag, *Nanoscale* **2018**, *10*, 9525.
[25] M. Lin, L. Chunlei, C. Fengyi, Y. Dehong, J. Xu, H. Sijie, M. Xiaomei, W. Pengfei, *Appl. Nano Mater.* **2019**, *2*, 2902.
[26] L. Xiao, J. Sun, L. Liu, R. Hu, H. Lu, C. Cheng, Y. Huang, S. Wang, J. Geng, *ACS Appl. Mater. Interfaces* **2017**, *9*, 5382.
[27] S. Omidi, A. Kakanejadifard, F. Azarbani, *J. Mol. Liq.* **2017**, *242*, 812.
[28] I. Barbolina, C. R. Woods, N. Lozano, K. Kostarelos, K. S. Novoselov, I. S. Roberts, *2D Mater.* **2016**, *3*, 025025.
[29] J. S. Dickson, M. Koohmaraie, *Appl. Environ. Microbiol.* **1989**, *55*, 832.
[30] B. Gottenbos, D. W. Grijpma, H. C. van der Mei, J. Feijen, H. J. Busscher, *J. Antimicrob. Chemother.* **2001**, *48*, 7.
[31] S. L. Walker, J. E. Hill, J. A. Redman, M. Elimelech, *Appl. Environ. Microbiol.* **2005**, *71*, 3093.
[32] R. Kügler, O. Bouloussa, F. Rondelez, *Microbiology* **2005**, *151*, 1341.
[33] H. Murata, R. R. Koepsel, K. Matyjaszewski, A. J. Russell, *Biomaterials* **2007**, *28*, 4870.
[34] S. Romero-Vargas Castrillón, F. Perreault, A. F. de Faria, M. Elimelech, *Environ. Sci. Technol. Lett.* **2015**, *2*, 112.
[35] L. Kan, Z. Xu, C. Gao, *Macromolecules* **2011**, *44*, 444.
[36] E. Kłodzinska, M. Szumski, E. Dziubakiewicz, K. Hrynkiewicz, E. Skwarek, W. Janusz, B. Buszewski, *Electrophoresis* **2010**, *31*, 1590.
[37] V. Bütün, S. P. Armes, N. C. Billingham, *Macromolecules* **2001**, *34*, 1148.
[38] J. Schindelin, I. Arganda-Carreras, E. Frise, V. Kaynig, M. Longair, T. Pietzsch, S. Preibisch, C. Rueden, S. Saalfeld, B. Schmid, J. Y. Tinevez, D. J. White, V. Hartenstein, K. Eliceiri, P. Tomancak, A. Cardona, *Nat. Methods* **2012**, *9*, 676.
[39] T. Naas, B. Coignard, A. Carbonne, K. Blanckaert, O. Bajolet, C. Bernet, X. Verdeil, P. Astagneau, J. C. Desenclos, P. Nordmann, *Emerging Infect. Dis.* **2006**, *12*, 1214.